EUROPEAN JOURNAL OF BIOMEDICAL AND PHARMACEUTICAL SCIENCES
http://www.ejbps.com

ISSN 2349-8870
Volume: 4
Issue: 2
177-186
Year: 2017

ISOTHERM ANALYSIS ON THE REMOVAL OF METHYLENE BLUE DYE FROM ARTIFICIAL WASTEWATER USING NANO-POROUS CARBON

A. Arasakumar and S. Arivoli*

PG and Research Department of Chemistry, Thiru Vi Ka Government Arts College, Thiruvarur, Tamilnadu, India.

***Corresponding Author: Dr. S. Arivoli**
PG and Research Department of Chemistry, Thiru Vi Ka Government Arts College, Thiruvarur, Tamilnadu, India.

Article Received on 07/12/2016 **Article Revised on 28/12/2016** **Article Accepted on 18/01/2017**

ABSTRACT
The use of low-cost, easily obtained and eco-friendly adsorbents has been employed as an ideal alternative to the current expensive methods of removing dyes from wastewater. This study investigates the potential use of activated nano carbon prepared from Pandanus Amaryllifolius Stem for the removal of methylene blue (MB) dye from simulated wastewater. The effect of pH, contact time, initial concentration and amount of adsorbent were considered. In order to investigate the mechanism of the adsorption process, several kinetic models including pseudo-first order, pseudo-second order, Elovich and intra-particle diffusion were used. In addition, equilibrium data was analyses to Langmuir, Freundlich, Temkin, Dubinin-Radushkevich, Hurkins-Jura, Halsay, Radlich-Peterson, Jovanovic and BET isotherm models. The obtained results showed that the adsorption of the methylene blue was enhanced with increasing initial dye concentration, pH and contact time. The optimum pH was 9. Considering the values of R^2 (0.999), BET isotherm model and pseudo-second order kinetic model had the best fitness.

KEYWORDS: Methylene Blue (MB), Activated Pandanus Amaryllifolius Stem Nano Carbon (APANC), Isotherm Models, Thermodynamic and Kinetic studies.

1. INTRODUCTION

One of the high consuming materials in the dye industry is methylene blue (MB) which is used for cotton and silk painting[1-4]. Chemical structure of MB is illustrated in the following. Up to now, a great number of methods have been proposed in order to remove dyes from the industrial wastewater among which adsorption is the most acceptable due to its cost effectiveness and its capability to be used in large scales[5].

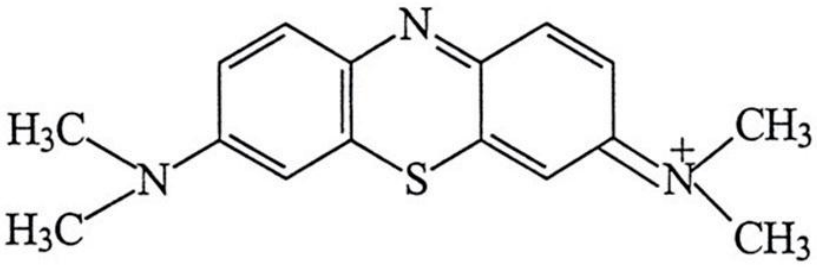

Molecular Structure of Methylene Blue

The methods of colour removal from industrial effluents include biological treatment, coagulation, flotation, adsorption, oxidation and hyper filtration[6]. Among the treatment options, adsorption has been found to be superior to other techniques for water treatment in terms of initial cost, simplicity of design, ease of operation and insensitivity of toxic substances.[7] Different adsorbents have been used for the removal of various materials from aqueous solutions, such as dyes, metal ions and other organic materials including perlite[8], bentonite[9], silica gels[10], fly ash[11], lignite[11], peat[12], silica[13], etc.

Among these natural materials, *Activated Pandanus Amaryllifolius Stem Nano Carbon* (APANC) which has a low weight and a fine micro-porous structure (up to 90%) and can be found in many regions of southern part

of TamilNadu, India. Because of its fine micro-porous structure, *Activated Pandanus Amaryllifolius Stem Nano Carbon* (APANC) has a high specific surface area and can float in water owing to its low density. Recently, many researchers have used Activated Carbon for removal of cadmium[14], disinfection by-products[15], heavy metals[16], sulfur dioxide[17] and azo dye[2].

2. MATERIALS AND METHODS

2.1 Instruments and Reagents

Stock solution was prepared by dissolving the required amount of MB in double distilled water. The test solutions were prepared by diluting stock solution to the desired concentrations. The concentration of the MB was determined at 620 nm. The pH measurements were done using Digital pH meter (Equip-Tronics EQ 614A, India) and adsorption studies were carried out on UV-Vis Double Beam spectrophotometer (Systronics 2203, India). All chemicals included NaOH, HCl and MB with the highest available purity and were purchased from Scientific Equipment Company, Tiruchirapalli, (Merck, All solutions were stirred on a hotplate and stirrer (JENWAY, model-1000, India).

2.2 Adsorbent Features

In the present experimental study, *Activated Pandanus Amaryllifolius Stem Nano Carbon* (APANC) samples as adsorbents were gathered from southern part of Tamil Nadu, India.

2.3 Preparing the Adsorbent

At first, Pandanus Amaryllifolius Stem was collected from local area of Thiruvarur district and washed several times by de-ionized water in order to remove the primary impurities. Next, the shell was placed in Con. H_2SO_4 (w/v) for 24 hours for carbonization and increasing the adsorbent's porosity. Afterwards, the prepared sample was washed several times by de-ionized water, ground well to fine powder and sieved by a mesh. Finally, this was activated around1200 ^{0}C in muffle furnace for 12 hours; the fine micro-porous size of activated nano carbon is 50 nm was utilized as the adsorbent.

2.4 Adsorption Study

To study the effect of important parameters like the pH, contact time and initial dye concentration on the adsorptive removal of MB, batch experiments were conducted. For each experimental run, 50 ml of different concentrations of the dye solution (25 - 125 mg/L) was agitated with 0.025 g of the adsorbent at 120 rpm until the equilibrium was achieved. Samples were withdrawn at different time intervals (15, 30, 45 and 60 minutes) and kinetics, isotherm and other parameters of adsorption was determined by analyzing the remaining dye concentration from aqueous solution. In order to evaluate the effect of the initial pH on MB adsorption, the equilibrium study was conducted at different pH levels 2, 3, 4, 5, 6, 7, 8 and 9 and other equilibrium studies were continued at the optimum pH 6.5. The pH of the solutions was adjusted by adding 0.01 N aqueous solutions of NaOH and HCl.

The percentage removal of dye was calculated using the following equation[18]:

$$\%\text{MB Removal} = \frac{(C_0 - C_t)}{C_0} \times 100 \quad \ldots\ldots\ldots (1)$$

Where, C_0 (mg/L) and C_t (mg/L) are the initial dye concentration and dye concentration at time t, respectively. When the system reached the equilibrium concentration, the equilibrium adsorption capacity was calculated through the following equation[19]:

$$q_e = \frac{v\,(C_0 - C_e)}{w} \quad \ldots\ldots\ldots\ldots\ldots (2)$$

In this equation, q_e (mg/g) represents the rate of the adsorbed dye per mass unit of the absorbent, C_0 (mg/L) and C_e (mg/L) are initial and equilibrium dye concentrations, respectively, and v (L) and w (g) are the volume of the dye solution and the weight of the adsorbent, respectively.

3. RESULTS AND DISCUSSION

3.1 The Effect of pH

Solution pH affects both aqueous chemistry and surface binding sites of the adsorbents. The effect of initial pH on adsorption of MB was studied from pH 2 to 9 at initial MB dye concentration of 25 mg/L, adsorbent dosage of 0.025 g and contact time of 60 min. Two possible mechanisms of adsorption of MB dye on the APANC adsorbent may be considered include: (a) electrostatic interaction between the adsorbent and the MB molecule, (b) a chemical reaction between the MB and the adsorbent. When pH increases, the concentration of OH^- ions in the desired solution is increased, as well. This causes the surface of the APANC to become deprotonated and, as a result, the negative charge of the used APANC surface will be amplified. Therefore, the electrostatic attractive force between the MB dye, which has a positive charge, and the adsorbent surface increases, and consequently, the rate of dye adsorption increases, as well[20] as Figure 3 depicts, as the pH of the solution increased from 2 to 9, the rate of removal also increased up to pH 6.5 then decrease.

3.2 The Effect of Contact Time

Generally, diffusion of the adsorbate on the used adsorbent and ultimately the adsorption phenomena on the adsorbent are time consuming processes[21]. The adsorption rate, obtained for MB adsorption on APANC was observed by decrease of the concentration of MB within the adsorption medium with contact time. The time necessary to reach the equilibrium for the removal of the MB molecules at different concentrations (25 - 125 mg/L) by APANC from aqueous solution was established to be about 60 minutes. As Figure 2 shows, at all the used concentrations, as the contact time between the adsorbent and the adsorbate increased, the adsorption rate increased, as well. According to Figure 2, the highest rate of MB removal took place during the 15 - 30 minute interval. In the remaining concentrations, this reduction continued up to 45 minutes with a lower slope. From this time up to 60 minutes, the system was almost constant and did not have much adsorption. At 25 mg/L of MB, the removal rate varied from 44.53% to 92.96% of the maximum removal onto APANC the values are shown in table 2. The surface of APANC may contain a large number of active sites and the solute uptake can be related to the active sites on equilibrium time. The higher sorption rate at the initial period (first 45 minutes) may be due to an increased number of vacant sites available at the initial stage. As a result there exists increased concentration gradient between adsorbate in solution and adsorbate in adsorbent surface. This increase in the concentration gradients tends to increase in MB sorption at the initial stages.

3.3 The Effect of Initial Concentration

The effect of the initial concentration of MB dye on the adsorption efficiency of the APANC was evaluated at different concentrations of 25, 50, 75, 100 and 125 mg/L. As Figure 1 depicts, one of the effective factors on the rate of dye uptake was the initial dye concentration of MB. In the present study, with the increase of the initial concentration from 25 mg/L to 125 mg/L, the rate of dye removal was reduced from 96.43% to 44.63% the values are shown in table 2. In addition, as the pollutant concentration increased in the aquatic environment, the number of available sites on the adsorbent surface decreased. In other words, with the decrease of the pollutant concentration in the aquatic environment, molecules of the adsorbate have more chance to react with the available active sites on APANC and, as a result, the adsorption rate is increased. Hence, one can claim that one method to increase the percentage of dye removal is dilution of wastewater[22].

3.4 Adsorption Isotherms

It is important to determine the most appropriate correlation for equilibrium adsorption isotherm, to optimize the design of a sorption system. The Freundlich, Langmuir, Temkin, Hurkins-Jura, Halsay, Redlich-Peterson, Dubinin-Radushkevich and Jovanovich isotherm models were used to analyses the adsorption equilibrium. Experimental isotherm data were obtained at an adsorption time of 60 min at different temperatures.

3.4.1 Freundlich adsorption isotherm

The Freundlich adsorption isotherm is based on the equilibrium sorption on heterogeneous surfaces. This isotherm is derived from the assumption that the adsorption sites are distributed exponentially with respect to heat of adsorption. The adsorption isotherm is expressed by the following equation

$$q_e = K_F C_e^{1/nF} \quad \ldots\ldots\ldots\ldots (3)$$

Which, can be linearized as

$$\ln q_e = \ln K_F + \frac{1}{n_F} \ln C_e \quad \ldots\ldots\ldots\ldots\ldots\ldots (4)$$

Where, q_e is the amount of MB dye adsorbed at equilibrium (mg/g) and C_e is the concentration of MB dye in the aqueous phase at equilibrium (ppm). K_F (L/g) and $1/n_F$ are the Freundlich constants related to adsorption capacity and sorption intensity, respectively.

The Freundlich constants K_F and $1/n_F$ were calculated from the slope and intercept of the $\ln q_e$ Vs $\ln C_e$ plot, the model parameters are shown in Table 3. The magnitude of K_F showed that APANC had a high capacity for MB dye adsorption from the aqueous solutions studied. The Freundlich exponent, n_F, should have values in the range of 1 and 10 (i.e., $1/n_F < 1$) to be considered as favourable adsorption[23]. A $1/n_F$ value of less than 1 indicated that MB dye is favorably adsorbed by APANC. The Freundlich isotherm did not show a good fit to the experimental data as indicated by SSE and Chi-square statistics.

3.4.2 Langmuir adsorption isotherm

The Langmuir adsorption isotherm is based on the assumption that all sorption sites possess equal affinity to the adsorbate. The Langmuir isotherm in a linear form can be represented as[23]:

$$\frac{C_e}{q_e} = \frac{1}{q_m K_L} + \frac{C_e}{q_m}$$

Where q_e is the amount of MB dye adsorbed at equilibrium (mg/g), C_e is the concentration of MB in the aqueous phase at equilibrium (ppm), q_m is the maximum MB dye uptake (mg/g), and K_L is the Langmuir constant related to adsorption capacity and the energy of adsorption (g/mg).

A linear plot of C_e/q_e Vs C_e was employed to determine the value of q_m and K_L, the data so obtained were also presented in Table 3. The model predicted a maximum value that could not be reached in the experiments. The value of K_L decreased with an increase in the temperature. A high K_L value indicates a high adsorption affinity. The monolayer saturation capacity, q_m, is shown to be 150.34, 162.28, 171.69 and 181.70 mg/g at a

temperature of 30, 40, 50 and 60°C, respectively. Weber and Chakraborti[24] expressed the Langmuir isotherm in term of dimensionless constant separation factor or equilibrium parameter (R_L) defined in the following equation:

$$R_L = \frac{1}{1+K_L C_0} \quad \text{..... (6)}$$

Where, C_0 is the initial MB dye concentration (ppm). Four scenarios can be distinguished:

The sorption isotherm is unfavorable when $R_L > 1$, the isotherm is linear when $R_L = 1$, The isotherm is favorable when $0 < R_L < 1$ and the isotherm is irreversible when $R_L = 0$. The values of dimensionless separation factor (R_L) for MB dye removal were calculated at different concentrations and temperatures. As shown in Table 4, at all concentrations and temperatures tested the values of R_L for MB dye adsorptions on the APANC were less than 1 and greater than zero, indicating favorable adsorption.

The Langmuir isotherm showed a better fit to the adsorption data than the Freundlich isotherm. The fact that the Langmuir isotherm fits the experimental data well may be due to homogeneous distribution of active sites on the APANC surface, since the Langmuir equation assumes that the adsorbent surface is energetically homogeneous.

3.4.3 Temkin adsorption isotherm

The Temkin adsorption isotherm assumes that the heat of adsorption decreases linearly with the sorption coverage due to adsorbent-adsorbate interactions.[25] The Temkin isotherm equation is given as:

$$q_e = \frac{RT}{bT} \ln(K_T C_e) \text{ .....(7)}$$

Which, can be represented in the following linear form

$$q_e = \frac{RT}{b} \ln K_T + \frac{RT}{b} \ln C_e \text{.....(8)}$$

Where, K_T (L/g) is the Temkin isotherm constant, b_T (J/mol) is a constant related to heat of sorption, R is the ideal gas constant (8.314 J/mol K), and T is absolute temperature (K). A plot of q_e versus $\ln C_e$ enables the determination of isotherm constants K_T and b_T from the slope and intercept, The model parameters are listed in Table 3. The Temkin isotherm appears to provide a good fit to the MB dye adsorption data.

The adsorption energy in the Temkin model, b_T, is positive for MB dye adsorption from the aqueous solution, which indicates that the adsorption is exothermic. The experimental equilibrium curve is close to that predicted by Temkin model. Consequently, the adsorption isotherm of MB dye on APANC can be described reasonably well by the Temkin isotherm.

3.4.4 Hurkins-Jura adsorption isotherm

The Hurkins-Jura adsorption isotherm can be expressed as [26]:

$$q_e = \sqrt{\frac{A_H}{B_H + \log C_e}} \text{.....(9)}$$

This can rearranged as follows:

$$\frac{1}{q_e^2} = \frac{B_H}{A_H} - \frac{1}{A_H} \log C_e \text{.....(10)}$$

Where, A_H (g^2/L) and B_H (mg^2/L) are two parameters characterizing the sorption equilibrium.

The isotherm equation accounts for multilayer adsorption and can be explained by the existence of a heterogeneous pore distribution. The Harkins–Jura isotherm parameters are obtained from the plots of of $1/q_e^2$ versus log C_e enables the determination of model parameters A_H and B_H from the slope and intercept.

3.4.5 Halsay adsorption isotherm

The Halsay adsorption isotherm can be given as [27]:

$$q_e = \exp\left(\frac{\ln K_{Ha} - \ln C_e}{n_{Ha}}\right) \text{.....(11)}$$

And, a linear form of the isotherm can be expressed as follows:

$$\ln q_e = \frac{\ln K_{Ha}}{n_{Ha}} - \frac{\ln C_e}{n_{Ha}} \text{.....(12)}$$

Where, K_{Ha} (mg/L) and n_{Ha} are the Halsay isotherm constants.

A plot of $\ln q_e$ Vs $\ln C_e$, enables the determination of n_{Ha} and K_{Ha} from the slope and intercept. This equation is suitable for multilayer adsorption and the fitting of the experimental data to this equation attest to the heteroporous nature of adsorbent. Fig. 9 also shows that the experimental data and the model predictions based on the non-linear form of the Halsay models. The model parameters are listed in Table 3. This result also shows that the adsorption of MB dye on APANC was not based on significant multilayer adsorption. The Halsay model is also not suitable to describe the adsorption of MB dye on APANC, because this model also assumes a multilayer behavior for the adsorption of adsorbate onto adsorbent.

3.4.6 Radlich-Peterson adsorption isotherm

The Radlich-Peterson adsorption isotherm contains three parameters and incorporates the features of Langmuir and Freundlich isotherms into a single equation. The general isotherm equation can be described as follows [28]:

$$q_e = \frac{K_R C_e}{1 + a_R C_e^g} \text{.....(13)}$$

The linear form of the isotherm can be expressed as follows:

$$\ln \frac{C_e}{q_e} = g \ln C_e - \ln K_R \text{.....(14)}$$

Where, K_R (L/g) and a_R (L/mg) are the Radlich-Peterson isotherm constants and g is the exponent between 0 and 1. There are two limiting cases: Langmuir form for g = 1 and Henry's law for g = 0.

A plot of ln C_e/q_e versus ln C_e enables the determination of isotherm constants g and K_R from the slope and intercept. The values of K_R, presented in Table 3, indicate that the adsorption capacity of the APANC decreased with an increase temperature. Furthermore, the value of g lies between 0 and 1, indicating favorable adsorption.

3.4.7 Dubinin-Radushkevich adsorption isotherm

The Dubinin-Radushkevich adsorption isotherm is another isotherm equation[32]. It is assumed that the characteristic of the sorption curve is related to the porosity of the adsorbent. The linear form of the isotherm can be expressed as follows [29]:

$$\ln q_e = \ln Q_D - B_D \left[RT \ln\left(1+\frac{1}{C_e}\right)\right]^2 \quad \text{.....(15)}$$

Where, Q_D is the maximum sorption capacity (mol/g), and B_D is the Dubinin-Radushkevich constant (mol^2/kJ^2). A plot of $\ln q_e$ Vs $R_T \ln(1+1/C_e)$ enables the determination of isotherm constants B_D and Q_D from the slope and intercept.

3.4.9 The Brunauer–Emmett–Teller (BET) isotherm model

Brunauer–Emmett–Teller (BET) [31] isotherm is a theoretical equation, most widely applied in the gas–solid equilibrium systems. It was developed to derive multilayer adsorption systems with relative concentration ranges from 25 to 125 mg/L corresponding to a monolayer coverage lying between 0.50 and 1.50. Its extinction model related to liquid–solid interface is exhibited as:

$$q_e = \frac{q_s C_{BET} C_e}{(C_s - C_e)[1+(C_{BET}-1)(C_e/C_s)]} \quad \text{.....(16)}$$

Where, CBET, Cs, qs and qe are the BET adsorption isotherm (L/mg), adsorbate monolayer saturation concentration (mg/L), theoretical isotherm saturation capacity (mg/g) and equilibrium adsorption capacity (mg/g), respectively. As C_{BET} and C_{BET} (C_e/C_s) is much greater than 1,

In the linear form as used is represented as

$$\frac{C_e}{q(C_s - C_e)} = \frac{1}{q_s C_{BET}} + \left(\frac{C_{BET}-1}{q_s C_{BET}}\right)\left(\frac{C_e}{C_s}\right) \quad \text{.....(17)}$$

Where, C_e is equilibrium Concentration (mg/l), C_s is adsorbate monolayer saturation concentration (mg/l) and C_{BET} is BET adsorption relating to the energy of surface interaction (l/mg)

3.5 Adsorption Kinetics

The rate and mechanism of the adsorption process can be elucidated based on kinetic studies. Dye adsorption on solid surface may be explained by two distinct mechanisms: (1) An initial rapid binding of dye molecules on the adsorbent surface; (2) relatively slow intra-particle diffusion. To analyze the adsorption kinetics of the dye, the pseudo-first-order, the pseudo-second-order, and intra-particle diffusion models were applied[32]. Each of these models and their linear modes of them equations presented in below.

Kinetic Models and Their Linear Forms

Model	Nonlinear Form	Linear Form	Number of Equation
Pseudo-first-order	$dq_t/d_t = k_1(q_e - q_t)$	$\ln(q_e - q_t) = \ln q_e - k_1 t$	(18)
Pseudo-second-order	$dq_t/d_t = k_2(q_e - q_t)^2$	$t/q_t = \frac{1}{k^2 q_e^2 + (1/q_e)t}$	(19)

Where, q_e and q_t refer to the amount of MB dye adsorbed (mg/g) at equilibrium and at any time, t (min), respectively and k_1 (1/min), k_2 (g/mg.min) are the equilibrium rate constants of pseudo-first order and pseudo-second order models, respectively. Pseudo-first order model is a simple kinetic model, which was proposed by Lagergren[33] during 1898 and is used for estimation of the surface adsorption reaction rate. The values of ln (q_e - q_t) were linearly correlated with t. The plot of ln (q_e - q_t) Vs t should give a linear relationship from which the values of k_1 were determined from the slope of the plot. In many cases, the first-order equation of Lagergren does not fit well with the entire range of contact time and is generally applicable over the initial stage of the adsorption processes[34].

In the pseudo-second order model[35], the slope and intercept of the t/q_t Vs t plot were used to calculate the second-order rate constant, k_2. The values of equilibrium rate constant (k_2) are presented in Table 6. According to Table 6, the value of R^2 (0.999) related to the pseudo-second order model revealed that MB dye adsorption followed this model, which is in agreement with the results obtained by Karagoz et al.[36] and Hameed et al.[37], Nevertheless, pseudo-first order and pseudo-second order kinetic models cannot identify the mechanism of diffusion of dye into the adsorbent pores.

3.5.1 Error analysis

The traditional methods of determining the isotherm parameters by linear regression appear to give a good fit to experimental data. However, the R^2 is based on the linear forms of the isotherm equations, but does not represent the errors in the isotherm curves. To evaluate the fit of the isotherm equations to the experimental data, different error functions of non-linear regression were used here to determine the constants model parameters, and they were compared with those determined from the less accurate linearized data fitting. The Sum of Square

Error (SSE) and chi-square test were used. SSE can be defined as[36, 37]

$$SSE=\sqrt{\Sigma\left(q_{e,exp}-q_{e,cal}\right)^2/N} \quad \text{.....(20)}$$

Where, $q_{e,cal}$ is the amount of sorbate adsorbed at equilibrium calculated from the model (mg g^{-1}), $q_{e,exp}$ is the equilibrium value obtained from experiment (mg g^{-1}) and N is the number of data points.

The chi-square test (χ^2) is basically the sum of the squared error of the differences between the experimental data and data obtained by calculating using the models, with each squared difference divided by the corresponding data obtained by calculating from models. This can be represented by Equation 20 [17]. If experimental data is fitted to the model, χ^2 should give a small number[18].

Nonlinear chi-square test (χ^2)

$$\chi^2=\Sigma\frac{\left(q_{e,cal}-q_e\right)^2}{q_{e,Cal}} \quad \text{.....(21)}$$

Nonlinear chi-square test is a statistical tool necessary for the best fit of an adsorption system, obtained by judging the sum squares differences between the experimental and the calculated data, with each squared difference is divided by its corresponding value (calculated from the models). Small χ^2 value indicates its similarities while a larger number represents the variation of the experimental data.

$$\chi^2=\Sigma\frac{\left(q_{e,cal}-q_e\right)^2}{q_{e,Cal}} \quad \text{.....(22)}$$

3.5.2 Simple Elovich Model

The simple Elovich model is expressed in the form,

$$q_t = \alpha + \beta \ln t \quad \text{.....(23)}$$

Where, q_t is the amount adsorbed at time t, α and β are the constants obtained from the experiment. A plot of q_t against ln t should give a linear relationship for the applicability of the simple Elovich kinetic. The figure shows the simple Elovich kinetics of MB dye on to APANC for various initial concentrations (25, 50, 75, 100 and 125 mg/L) of volume 50 mL (each), adsorbent dose 0.025g, temperature 30 ^oC and pH 6.5. Their related parameters are listed in Table 6.

3.5.3 Intra-Particle Diffusion Model

The adsorption process on a porous adsorbent is generally a multi-step process. In order to analyse the mechanism of the adsorption of MB dye by APANC, the experimental data were tested against the intra-particle diffusion model. The adsorption mechanism of the adsorbate on to the adsorbent follows three consecutive steps: mass transfer across the external film of liquid surrounding the particle, adsorption at the surface of pores and the intra-particle diffusion. The slowest of these steps determines the overall rate of the process. The possibility of intraparticle diffusion resistance which could affect the adsorption is explored by using the intra-particle diffusion model given in the equation,

$$q_t = K\,t^{1/2} + I \quad \text{.....(24)}$$

Where, K is the intra-particle diffusion rate constant and I is the intercept. A plot of q_t against $t^{1/2}$ is drawn to analyse the possibility of intra-particle diffusion as the rate determining step. A two stage adsorption mechanism with first was rapid and second was slow has been observed from the experimental data. The plot of q_t against $t^{1/2}$ is multi-linear and deviating from the origin, indicating more than one process has affected the adsorption[18]. Hence, the first portion of the plot indicates the external mass transfer and the second portion is due to intra-particle or pore diffusion.

3.6 Thermodynamic treatment of the sorption process

In order to study the feasibility of the adsorption process, the thermodynamic parameters such as free energy, enthalpy and entropy changes can be estimated from the following equations.

$$K_c = C_{Ae}/C_e \quad \text{.....(25)}$$

$$\Delta G^0 = -RT \ln K_c \quad \text{.....(26)}$$

$$\text{Log } K_c = \Delta S^0/2.303R - \Delta H^0/2.303RT \quad \text{.....(27)}$$

Where C_e is the equilibrium concentration in solution in mg/L and C_{Ae} is the equilibrium concentration on the sorbent in mg/L and K_c is the equilibrium constant. The Gibbs free energy (ΔG^0) for the adsorption of MB onto biomass at all temperatures was obtained from Eq.26 and is presented in Table 5. The values of ΔH^0 and ΔS^0 were calculated from the slope and intercept of the plot log K_c against 1/T. Their related parameters are also listed in Table 5.

In order to support that physical adsorption is the predominant mechanism, the values of activation energy (Ea) and sticking probability (S*) were calculated from the experimental data. They were calculated using modified Arrhenius type equation related to surface coverage (θ) as follows[49]:

$$\theta = \left(1-\frac{C_e}{C_i}\right) \quad \text{.....(28)}$$

$$S^* = (1-\theta)_e\,\frac{-E_a}{RT} \quad \text{.....(29)}$$

The sticking probability, S*, is a function of the adsorbate/adsorbent system under consideration but must satisfy the condition $0 < S^* < 1$ and is dependent on the temperature of the system. The values of Ea and S* can be calculated from slope and intercept of the plot of ln(1-θ) versus 1/T respectively and are listed in Table 5.

From Table 5 it is clear that the reaction is spontaneous in nature as ΔG^0 values are negative at all the temperature studied. Again positive ΔH^0 value confirms that the sorption is endothermic in nature. The positive value of ΔS^0reflects the affinities of the adsorbents for the MB dye. The result as shown in Table 5 indicate that the probability of the MB dye to stick on surface of biomass is very high as S*<< 1, these values confirm that, the sorption process is physisorption.

TABLE: 2. EQUILIBRIUM PARAMETERS FOR THE ADSORPTION OF MB DYE ONTO APANC

M_0	C_e (Mg / L)				Q_e (Mg / L)				Removal %			
	30°C	40°C	50°C	60°C	30°C	40°C	50°C	60°C	30°C	40°C	50°C	60°C
25	3.6582	2.9010	2.6585	2.4625	46.685	47.198	46.683	47.075	93.37	94.306	94.996	95.150
50	8.2625	6.1075	5.3360	4.2975	85.475	87.785	89.328	91.405	85.542	87.785	89.311	91.021
75	17.276	14.970	13.763	12.445	117.44	120.05	122.47	125.11	78.052	80.039	81.648	83.406
100	34.937	31.447	29.181	26.577	132.12	137.10	141.63	146.84	66.062	68.552	70.819	73.423
125	46.558	50.774	46.387	41.556	137.56	148.45	157.22	166.88	55.025	59.380	62.65	66.755

TABLE: 3. ISOTHERMS PARAMETER FOR THE ADSORPTION OF MB DYE ONTO APANC

Model	Constant	Temperature (°C)			
		30	40	50	60
Freundlich	K_f (mg/g) (L/mg)$^{1/n}$	43.386	41.390	43.565	46.497
	n	2.2215	2.8475	2.8046	2.7682
Langmuir	Q_m (mg/g)	1210.34	132.28	151.09	163.11
	K_L (L/mg)	0.2006	0.1972	0.1943	0.2078
Temkin	b_T (J/mol)	22.220	31.360	32.934	34.667
	K_T (L/mg)	1.0098	1.0235	1.4868	1.5824
Hurkins-Jura	A_H (g^2/L)	-3167.7	-3529.4	-3207.8	-3808.1
	B_H (mg^2/L)	-1.6773	-1.6385	-1.5640	-1.5406
Halsay	K_{Ha} (mg/L)	46410.5	40199.8	39557.4	41298.8
	n_{Ha}	2.9251	2.8475	2.8046	2.7682
Radlich-Peterson	g	0.6581	0.6488	0.6434	0.6387
	K_R (L/g)	0.0253	0.0241	0.0229	0.0215
Dubinin-Radushkevich	q_s (mg/g)	121.39	127.12	131.52	137.71
	$K_D \times 10^{-4}$ mol^2 kJ^{-2}	1.5674	1.5750	1.5801	1.5876
Jovanovic	K_J (L/g)	0.0160	0.0189	0.0216	0.0250
	q_{max} (mg/g)	62.409	63.028	64.640	65.525
BET	C_{BET} (L/mg)	-4.3541	-19.871	-111.27	90.371
	qs (mg/g)	-0.2304	-0.0522	-0.0086	0.0111

TABLE: 4. DIMENSIONLESS SEPERATION FACTOR (R_L) FOR THE ADSORPTION OF MB DYE ONTO APANC

(C_i)	Temperature °C			
	30°C	40°C	50°C	60°C
25	0.0762	0.1545	0.1878	0.1613
50	0.0906	0.0933	0.0520	0.0877
75	0.0872	0.0242	0.0633	0.0602
100	0.0474	0.0489	0.0482	0.0458
125	0.0383	0.0395	0.0389	0.0370

TABLE: 5. THERMODYNAMIC PARAMETER FOR THE ADSORPTION OF MB DYE ONTO APANC

(C_0)	ΔG^o				$\Delta H°$	$\Delta S°$	Ea	S^*
	30°C	40°C	50°C	60°C				
25	-5879.35	-6878.96	-7871.11	-7542.3	-11.766	58.413	10923.3	9×10^{-3}
50	-4484.81	-5847.29	-5875.69	-6545.21	-16.141	67.936	14506.5	0.7×10^{-3}
75	-3542.45	-3613.93	-4008.59	-4540.47	-9.2025	40.986	7465.73	1.3×10^{-3}
100	-1677.95	-2027.91	-2380.92	-2813.39	-9.6970	37.490	6766.95	1.3×10^{-3}
125	-508.124	-988.122	-1416.56	-1930.06	-13.704	46.902	8124.04	1.5×10^{-3}

TABLE: 6. THE KINETIC PARAMETERS FOR THE ADSORPTION OF MB DYE ONTO APANC

C_0	Temp °C	Pseudo second order				Elovich model			Intraparticle diffusion		
		q_e	k_2	γ	h	α	β	γ	K_{id}	γ	C
25	30	43.506	0.0017	0.9983	4.9212	15.026	0.0977	0.9923	0.2704	0.9964	1.6820
	40	40.326	0.0030	0.9960	7.7923	136.77	0.1579	0.9951	0.1535	0.9939	1.5535
	50	40.850	0.0030	0.9940	7.8878	146.00	0.1578	0.9976	0.1517	0.9943	1.5729
	60	41.025	0.0032	0.9946	8.3582	208.44	0.1652	0.9987	0.1428	0.9937	1.5835
50	30	97.751	0.0010	0.9988	10.354	43.428	0.0593	0.9967	0.2325	0.9981	1.6107
	40	96.443	0.0014	0.9954	13.714	169.95	0.0773	0.9989	0.1664	0.9981	1.6476
	50	97.820	0.0014	0.9990	14.325	202.16	0.0781	0.9984	0.1613	0.9964	1.6570
	60	99.494	0.0015	0.9987	15.543	276.60	0.0800	0.9967	0.1530	0.9948	1.6820
75	30	130.94	0.0009	0.9967	16.070	129.76	0.0521	0.9983	0.1870	0.9971	1.5535
	40	133.12	0.0009	0.9961	17.114	152.36	0.0523	0.9943	0.1816	0.9932	1.5729
	50	135.82	0.0009	0.9981	17.454	159.29	0.0515	0.9982	0.1805	0.9946	1.5835
	60	137.92	0.0009	0.9975	18.848	213.31	0.0531	0.9972	0.1704	0.9923	1.6107
100	30	151.69	0.0006	0.9969	14.521	67.580	0.0393	0.9969	0.2267	0.9951	1.4074
	40	156.39	0.0006	0.9973	15.794	78.632	0.0388	0.9981	0.2202	0.9976	1.4362
	50	160.10	0.0006	0.9989	17.287	100.25	0.0394	0.9948	0.2081	0.9964	1.4716
	60	165.01	0.0006	0.9928	18.631	123.26	0.0395	0.9994	0.1992	0.9971	1.5028
125	30	151.80	0.0008	0.9941	18.710	148.62	0.0447	0.9972	0.1879	0.9941	1.3950
	40	170.51	0.0005	0.9948	16.089	69.824	0.0343	0.9963	0.2329	0.9964	1.3501
	50	181.60	0.0005	0.9959	16.643	69.595	0.0318	0.9987	0.2370	0.9939	1.3682
	60	190.17	0.0005	0.9941	19.113	98.637	0.0322	0.9956	0.2177	0.9924	1.4277

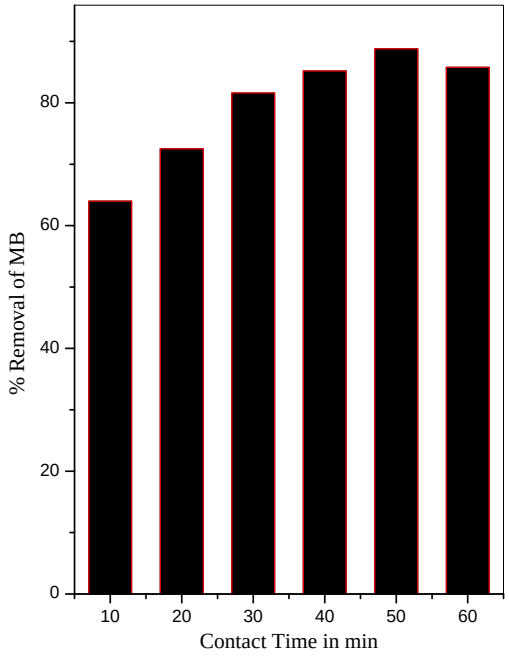

Fig:2- Effect of Contact Time on the Removal of MB Dye
[MB]=50 mg/L;Temprature 30°C;Adsorbent dose=0.025g/50ml

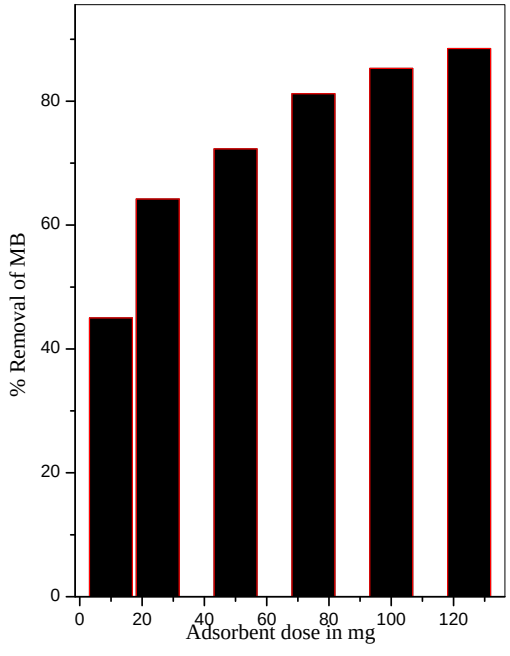

Fig;1- Effect of Adsorbent dose on the removal of MB Dye
[MB]=50mg/L;Contact Time 60 min;Temprature 30°C

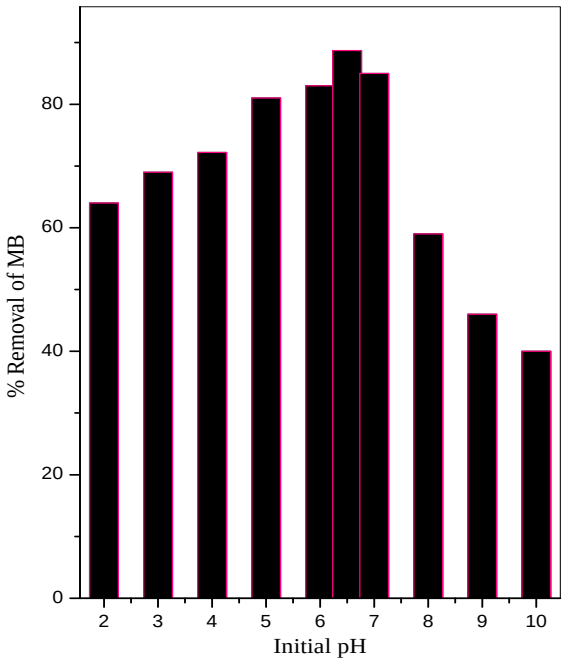

Fig;3- Effect of Initial pH on the removal of MB Dye
[MB]=50 mg/L;Temprature 30^{o}C;Adsorbent dose=0.025g/50ml

4. DISCUSSION

The present study investigated the efficiency of APANC as a cheap adsorbent and the results revealed that APANC was an appropriate adsorbent for removing MB from the aquatic environments. pH also plays a major role in removing the MB. The findings of the present study also showed that as the contact time increased, the dye's primary concentration as well as the dose of the intended adsorbate of the adsorption efficiency increased, as well. Adsorption equilibrium data follows Langmuir, Freundlich, Temkin, Dubinin-Radushkevich, Hurkins-Jura, Halsay, Radlich-Peterson, Jovanovic and BET isotherm models. The equilibrium data fitted very well in the Langmuir and BET isotherm equation. The kinetic study of MB on to APANC was performed based on pseudo-first-order, pseudo-second-order and intra-particle diffusion equations. The data indicate that the adsorption kinetics follow the pseudo-second-order rate. This study concludes that the APANC could be em-ployed as an appropriate, inexpensive, accessible and low-cost adsorbent for the removal of MB from aquatic environments.

REFERENCES

1. Sapci Z, Ustun B. The removal of color and COD from textile wastewater by using waste pumice. Elec J Environ Agric Food Chem. 2003; 2(2): 286–90.
2. Samarghandi MR, Zarrabi M, Sepehr MN, Amrane A, Safari GH, Bashiri S. Application of acidic treated pumice as an adsorbent for the removal of azo dye from aqueous solutions: kinetic, equilibrium and thermodynamic studies. Iranian J Environ Health Sci Eng. 2012; 9(1): 9.
3. Iqbal MJ, Ashiq MN. Adsorption of dyes from aqueous solutions on activated charcoal. J Hazard Mater. 2007; 139(1): 57–66.
4. Yang J, Qiu K. Preparation of activated carbons from walnut shells via vacuum chemical activation and their application for methylene blue removal. Chem Eng J. 2010; 165(1): 209–17.
5. Robinson T, McMullan G, Marchant R, Nigam P. Remediation of dyes in textile effluent: a critical review on current treatment technologies with a proposed alternative. Bioresour Technol. 2001; 77(3): 247–55.
6. Santhy K, Selvapathy P. Removal of reactive dyes from wastewater by adsorption on coir pith activated carbon. Bioresour Technol. 2006; 97(11): 1329–36.
7. McKay G, Porter JF, Prasad GR. The removal of dye colours from aqueous solutions by adsorption on low-cost materials. Water Air Soil Pollut. 1999; 114(3-4): 423–38.
8. Doğan M, Alkan M, Onganer Y. Adsorption of methylene blue from aqueous solution onto perlite. Water Air Soil Pollut. 2000; 120(3-4): 229–48.
9. Bereket G, Aro AZ, ozel MZ. Removal of Pb(II), Cd(II), Cu(II), and Zn(II) from Aqueous Solutions by Adsorption on Bentonite. J Colloid Interface Sci. 1997; 187(2): 338–43.
10. Mohamed MM. Adsorption properties of ionic surfactants on molybdenum-modified silica gels. Colloids Surf A: Physicochem Eng Aspect. 1996; 108(1): 39–48.
11. Mohan D, Singh KP, Singh G, Kumar K. Removal of dyes from wastewater using flyash, a low-cost adsorbent. Indust Eng chem Res. 2002; 41(15): 3688–95.

12. Ho Y, McKay G. Sorption of dye from aqueous solution by peat. Chem Eng J. 1998; 70(2): 115–24.
13. McKay G, Otterburn MS, Sweeney AG. Surface mass transfer processes during colour removal from effluent using silica. Water Res. 1981; 15(3): 327–31.
14. Panuccio MR, Sorgona A, Rizzo M, Cacco G. Cadmium adsorption on vermiculite, zeolite and pumice: batch experimental studies. J Environ Manage. 2009; 90(1): 364–74.
15. Kaplan Bekaroglu SS, Yigit NO, Karanfil T, Kitis M. The adsorptive removal of disinfection by-product precursors in a high-SUVA water using iron oxide-coated pumice and volcanic slag particles. J Hazard Mater. 2010; 183(1-3): 389–94.
16. Moraci N, Calabro PS. Heavy metals removal and hydraulic performance in zero-valent iron/pumice permeable reactive barriers. J Environ Manage. 2010; 91(11): 2336–41.
17. Ozturk B, Yildirim Y. Investigation of sorption capacity of pumice for SO 2 capture. Process Safety Environ Protec. 2008; 86(1): 31–6.
18. Yavuz Ö, Aydin AH. Removal of direct dyes from aqueous solution using various adsorbents. Polish J Environ Studies. 2006; 15(1): 155– 61.
19. Alkan M, Doğan M. Adsorption of copper (II) onto perlite. J Colloid Interface Sci. 2001; 243(2): 280–91.
20. Han R, Wang Y, Han P, Shi J, Yang J, Lu Y. Removal of methylene blue from aqueous solution by chaff in batch mode. J Hazard Mater. 2006; 137(1): 550–7.
21. El Qada EN, Allen SJ, Walker GM. Adsorption of methylene blue onto activated carbon produced from steam activated bituminous coal: a study of equilibrium adsorption isotherm. Chem Eng J. 2006; 124(1): 103–10.
22. Chen H, Zhao J, Dai G. Silkworm exuviae--a new non-conventional and low-cost adsorbent for removal of methylene blue from aqueous solutions. J Hazard Mater. 2011; 186(2-3): 1320–7.
23. Karagoz S, Tay T, Ucar S, Erdem M. Activated carbons from waste biomass by sulfuric acid activation and their use on methylene blue adsorption. Bioresour Technol. 2008; 99(14): 6214–22.
24. Hameed BH, Din AT, Ahmad AL. Adsorption of methylene blue onto bamboo-based activated carbon: kinetics and equilibrium studies. J Hazard Mater. 2007; 141(3): 819–25.
25. Rao GB, Kalyani G, Saradhi BV, Kumar YP. Removal of Fluoride from Aqueous Solution Using a Waste Material. Nature Environ Pollut Tech. 2009; 8(2): 231–6.
26. Removal of Rhodamine B dye from aqueous solution using the acid activated Cynodon dactylon carbon. BR Venkatraman, U Gayathri, S Elavarasi, S Arivoli Der Chemica Sinica 3(1).
27. Isolation and Characterization of Flavonoids from Chloroxylon Swietenia R Prabakaran, S Arivoli, A Hema, C Kamatchi, J Chem Pharm Res 3(3): 805.